

Metabolomic Profiling of Anionic Metabolites by Capillary Electrophoresis Mass Spectrometry

Tomoyoshi Soga,^{*,†} Kaori Igarashi,[†] Chiharu Ito,[†] Katsuo Mizobuchi,[‡] Hans-Peter Zimmermann,[§] and Masaru Tomita[†]

Institute for Advanced Biosciences, Keio University, Tsuruoka, Yamagata 997-0052, Japan, Agilent Technologies, 9-1 Takakura-cho, Hachioji, Tokyo 192-8510, Japan, and Agilent Technologies, Hewlett-Packard-Strasse 8, 76337 Waldbronn, Germany

We describe a sheath flow capillary electrophoresis time-of-flight mass spectrometry (CE-TOFMS) method in the negative mode using a platinum electrospray ionization (ESI) spray needle, which allows the comprehensive analysis of anionic metabolites. The material of the spray needle had significant effect on the measurement of anions. A stainless steel spray needle was oxidized and corroded at the anodic electrode due to electrolysis. The precipitation of iron oxides (rust) plugged the capillary outlet, resulting in shortened capillary lifetime. Many anionic metabolites also formed complexes with the iron oxides or migrating nickel ion, which was also generated by electrolysis and moved toward the cathode (the capillary inlet). The metal–anion complex formation significantly reduced detection sensitivity of the anionic compounds. The use of a platinum ESI needle prevented both oxidation of the metals and needle corrosion. Sensitivity using the platinum needle increased from several- to 63-fold, with the largest improvements for anions exhibiting high metal chelating properties such as carboxylic acids, nucleotides, and coenzyme A compounds. The detection limits for most anions were between 0.03 and 0.87 $\mu\text{mol/L}$ (0.8 and 24 fmol) at a signal-to-noise ratio of 3. This method is quantitative, sensitive, and robust, and its utility was demonstrated by the analysis of the metabolites in the central metabolic pathways extracted from mouse liver.

Metabolism is the entire network of chemical reactions that occur in a cell in order to maintain life, in which one metabolite is transformed into another by a sequence of enzymes. Among the whole cellular metabolic network, central carbon metabolism, composed of glycolysis, the pentose phosphate pathway, and the tricarboxylic acid (TCA) cycle, plays key functions in substrate degradation, energy and cofactor regeneration, and biosynthetic precursor supply (DNA, RNA, proteins, peptidoglycan, and lipid bilayers).^{1,2} Interestingly, all the components involved in the central carbon and energy metabolism are negatively charged: phosphorylated saccharides, phosphorylated carboxylic acids,

carboxylic acids, coenzyme A (CoA) compounds, nucleotides, and nicotinamide adenine dinucleotides.

As the importance of metabolomics is recognized, several large-scale metabolite analysis methods using GC/MS,³ LC/MS,^{2,4,5} NMR^{6–8} or Fourier transform ion cyclotron resonance mass spectrometry (FTICR-MS)^{9,10} have been developed. However, only a limited number of methodologies enable the simultaneous analysis of the anionic metabolites due to their extremely large physicochemical diversity.

Recently, approaches based on capillary electrophoresis mass spectrometry (CE-MS)^{11,12} and CE time-of-flight mass spectrometry (CE-TOFMS)¹³ have emerged as powerful tools for the comprehensive analysis of charged metabolites and have played a critical role in understanding intricate biochemical and biological systems.^{13–19}

- (1) Sonenshein, A. L. *Nat. Rev. Microbiol.* **2007**, *5*, 917–927.
- (2) Yang, W. C.; Sedlak, M.; Regnier, F. E.; Mosier, N.; Ho, N.; Adamec, J. *Anal. Chem.* **2008**, *80*, 9508–9516.
- (3) Fiehn, O.; Kopka, J.; Dormann, P.; Altmann, T.; Trethewey, R. N.; Willmitzer, L. *Nat. Biotechnol.* **2000**, *18*, 1157–1161.
- (4) Plumb, R.; Granger, J.; Stumpf, C.; Wilson, I. D.; Evans, J. A.; Lenz, E. M. *Analyst* **2003**, *128*, 819–823.
- (5) Yoshida, H.; Mizukoshi, T.; Hirayama, K.; Miyano, H. *J. Agric. Food Chem.* **2007**, *55*, 551–560.
- (6) Reo, N. V. *Drug Chem. Toxicol.* **2002**, *25*, 375–382.
- (7) Coen, M.; Lenz, E. M.; Nicholson, J. K.; Wilson, I. D.; Pognan, F.; Lindon, J. C. *Chem. Res. Toxicol.* **2003**, *16*, 295–303.
- (8) Coen, M.; Ruepp, S. U.; Lindon, J. C.; Nicholson, J. K.; Pognan, F.; Lenz, E. M.; Wilson, I. D. *J. Pharm. Biomed. Anal.* **2004**, *35*, 93–105.
- (9) Aharoni, A.; Ric de Vos, C. H.; Verhoeven, H. A.; Maliepaard, C. A.; Kruppa, G.; Bino, R.; Goodenowe, D. B. *Omics* **2002**, *6*, 217–234.
- (10) Hirai, M. Y.; Yano, M.; Goodenowe, D. B.; Kanaya, S.; Kimura, T.; Awazuhara, M.; Arita, M.; Fujiwara, T.; Saito, K. *Proc. Natl. Acad. Sci. U.S.A.* **2004**, *101*, 10205–10210.
- (11) Soga, T.; Ohashi, Y.; Ueno, Y.; Naraoka, H.; Tomita, M.; Nishioka, T. *J. Proteome Res.* **2003**, *2*, 488–494.
- (12) Edwards, J. L.; Chisom, C. N.; Shackman, J. G.; Kennedy, R. T. *J. Chromatogr., A* **2006**, *1106*, 80–88.
- (13) Soga, T.; Baran, R.; Suematsu, M.; Ueno, Y.; Ikeda, S.; Sakurakawa, T.; Kakazu, Y.; Ishikawa, T.; Robert, M.; Nishioka, T.; Tomita, M. *J. Biol. Chem.* **2006**, *281*, 16768–16776.
- (14) Ishii, N.; Nakahigashi, K.; Baba, T.; Robert, M.; Soga, T.; Kanai, A.; Hirasawa, T.; Naba, M.; Hirai, K.; Hoque, A.; Ho, P. Y.; Kakazu, Y.; Sugawara, K.; Igarashi, S.; Harada, S.; Masuda, T.; Sugiyama, N.; Togashi, T.; Hasegawa, M.; Takai, Y.; Yugi, K.; Arakawa, K.; Iwata, N.; Toya, Y.; Nakayama, Y.; Nishioka, T.; Shimizu, K.; Mori, H.; Tomita, M. *Science* **2007**, *316*, 593–597.
- (15) Ohashi, Y.; Hirayama, A.; Ishikawa, T.; Nakamura, S.; Shimizu, K.; Ueno, Y.; Tomita, M.; Soga, T. *Mol. Biosyst.* **2008**, *4*, 135–147.
- (16) Yoshida, S.; Imoto, J.; Minato, T.; Oouchi, R.; Sugihara, M.; Imai, T.; Ishiguro, T.; Mizutani, S.; Tomita, M.; Soga, T.; Yoshimoto, H. *Appl. Environ. Microbiol.* **2008**, *74*, 2787–2796.

* To whom correspondence should be addressed. Phone: (+81) 235 29 0528. Fax: (+81) 235 29 0574. E-mail: soga@sfc.keio.ac.jp.

[†] Keio University.

[‡] Agilent Technologies, Japan.

[§] Agilent Technologies, Germany.

Application of the sheath flow CE-MS to the analysis of anionic metabolites has been successfully performed using the “negative mode” and a cationic polymer coated capillary.²⁰ This methodology reverses electroosmotic flow (EOF)²¹ toward the anode (the MS direction) to prevent a deleterious current drop. The method enabled the large-scale determination of anionic metabolites, however, with limitations. Several anionic metabolites such as citrate, nucleotides, and CoA compounds were not detected or were detected as poorly shaped peaks.^{20,22,23} To overcome the problem, a pressure-assisted CE-MS method²⁴ was used for these analytes.^{22,23} While successful, two separate CE-MS methods for anions were necessary,¹¹ and moreover, these approaches were not ideal. Additionally, the capillaries frequently clogged.

Recently, it was found that these problems were caused by metal ions generated from the stainless steel needle of the electrospray ionization (ESI) sprayer. Iron oxides formed at the capillary outlet, while nickel ions migrated into the separation capillary and formed complexes with many anions. Here, we propose an improved sheath flow CE-MS method for the analysis of anionic metabolites using a platinum ESI spray needle. The platinum material has a low ionization tendency and does not generate metal ions through electrolysis. This approach overcame the problems and provided robust and sensitive analysis of most of the anionic metabolites and was successfully applied to the quantitative analysis of mouse hepatic metabolites in the central carbon and energy metabolic pathways.

EXPERIMENTAL SECTION

Chemicals. Glycerophosphate was purchased from Nacal Tesque (Kyoto, Japan), 2-morpholinoethanesulfonate (MES, internal standard) from Dojindo (Kumamoto, Japan), and hexakis-(2,2-difluorothoxy)-phosphazene (Hexakis) from SynQuest Laboratories (Alachua, FL). All other reagents were obtained from Sigma-Aldrich (St. Louis, MO) or Wako (Osaka, Japan). Individual stock solutions of carboxylic acids, phosphorylated saccharides, and phosphorylated carboxylic acids were prepared at a concentration of 100 mM, and stock solutions for other compounds of 10 mM were prepared in Milli-Q water, except for fumarate and trimesate (reference peak) which were prepared in 0.1 M NaOH and succinyl CoA which was prepared in 0.1 M HCl. The working mixture standard was prepared by diluting these stock solutions with Milli-Q water just before injection. All chemicals were of analytical or reagent grade. Water was purified with a Milli-Q purification system (Millipore, Bedford, MA).

Metabolite Extraction. Liver tissue (approximately 300 mg) was immediately plunged into methanol (1 mL) containing 300 μ M each of L-methionine sulfone and 2-morpholinoethanesulfonate

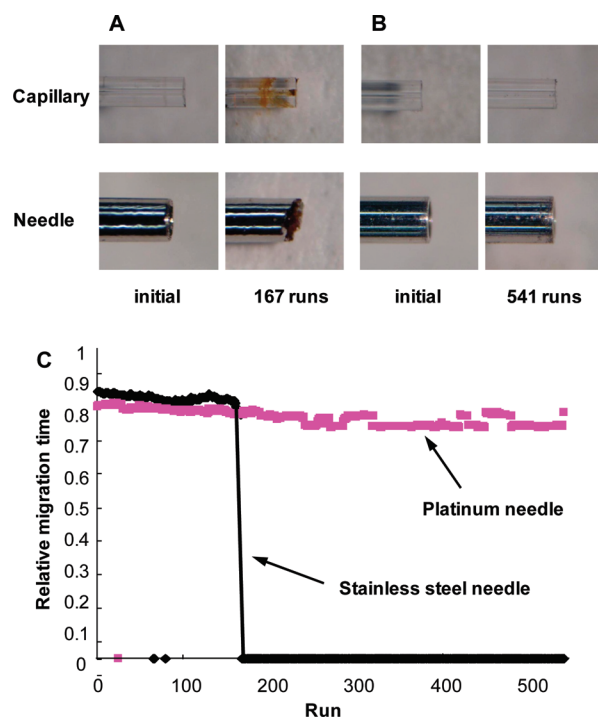


Figure 1. Robustness of the CE-TOFMS system in the anion standard analysis. Photograph of the capillary outlet and the tip of the needle of the COSMO(+) capillary obtained by the CE-ESI-MS sprayer with (A) the SSTS316Ti stainless steel needle and (B) the platinum needle. (C) Endurance of the system between the SSTS316Ti stainless steel needle (black) and platinum needle (magenta). The endurance was expressed using the relative migration time of lactate, which was calculated by normalization with the migration time of MES (internal standard). Experimental conditions are described in the Experimental Section.

(MES) (internal standards) and homogenized for 2 min to inactivate enzymes. Then Milli-Q water (500 μ L) was added, 300 μ L of the solution was transferred, and 200 μ L of chloroform was added and mixed well. The solution was centrifuged at 15 000 rpm for 15 min at 4 °C, and the separated 200 μ L aqueous layer was centrifugally filtered through a Millipore 5 kDa cutoff filter to remove proteins. The filtrate (100 μ L) was lyophilized and dissolved in 50 μ L of Milli-Q water containing reference compounds (200 μ M each of trimesate and 3-aminopyrrolidine). The solution (2 μ M) was diluted with 18 μ L of Milli-Q water and then injected into the CE-TOFMS system.¹³

Instrumentation. All CE-ESI-MS experiments were performed using an Agilent CE capillary electrophoresis system, an Agilent G3250AA LC/MSD TOF system, an Agilent1100 series isocratic HPLC pump, a G1603A Agilent CE-MS adapter kit, and a G1607A Agilent CE-ESI-MS sprayer kit (Agilent Technologies, Waldbronn, Germany). The CE-MS adapter kit includes a capillary cassette which facilitates thermostating of the capillary, and the CE-ESI-MS sprayer kit which simplifies coupling the CE system with MS systems was equipped with an electrospray source. For system control and data acquisition, we used G2201AA Agilent ChemStation software for CE and Agilent TOF (Analyst QS) software for TOFMS.

In addition, the original Agilent SSTS316Ti stainless steel (Fe/Cr/Ni/Mo/Ti; 68:18:11:2:1) ESI needle was replaced with passivated SSTS316Ti stainless steel (with 1% formic acid and 20%

- (17) Sato, S.; Soga, T.; Nishioka, T.; Tomita, M. *Plant J.* **2004**, *40*, 151–163.
- (18) Kinoshita, A.; Tsukada, K.; Soga, T.; Hishiki, T.; Ueno, Y.; Nakayama, Y.; Tomita, M.; Suematsu, M. *J. Biol. Chem.* **2007**, *282*, 10731–10741.
- (19) Williams, B. J.; Cameron, C. J.; Workman, R.; Broeckling, C. D.; Sumner, L. W.; Smith, J. T. *Electrophoresis* **2007**, *28*, 1371–1379.
- (20) Soga, T.; Ueno, Y.; Naraoka, H.; Ohashi, Y.; Tomita, M.; Nishioka, T. *Anal. Chem.* **2002**, *74*, 2233–2239.
- (21) Lukacs, K. D.; Jorgenson, J. W. *J. High Resolut. Chromatogr. Chromatogr. Commun.* **1985**, *8*, 407–411.
- (22) Soga, T.; Ueno, Y.; Naraoka, H.; Matsuda, K.; Tomita, M.; Nishioka, T. *Anal. Chem.* **2002**, *74*, 6224–6229.
- (23) Soga, T.; Ishikawa, T.; Igarashi, S.; Sugawara, K.; Kakazu, Y.; Tomita, M. *J. Chromatogr., A* **2007**, *1159*, 125–133.
- (24) Cao, P.; Moini, M. *Electrophoresis* **1998**, *19*, 2200–2206.

Table 1. Reproducibility, Linearity, and Sensitivity

compound	RSD (<i>n</i> = 8) (%)		linearity correlation	detection limit (μmol/L)	improved sensitivity ratio ^a
	migration time	peak area			
glyoxylate	0.6	11.1	0.997	8.0	0.9
glycolate	0.6	12.4	0.997	5.2	1.7
pyruvate	0.5	8.8	0.999	9.5	0.8
lactate	0.6	5.7	0.985	2.9	1.1
fumarate	0.5	9.4	0.989	0.32	1.4
succinate	0.5	6.3	0.999	0.23	1.6
malate	0.5	4.5	0.994	0.14	4.5
2-oxoglutarate	0.5	5.3	0.985	0.73	4.9
cysteine sulfinate	0.6	6.5	0.998	0.36	4.0
PEP	0.5	5.2	0.995	0.12	3.0
DHAP	0.6	7.8	0.998	0.40	2.2
glycerophosphate	0.6	8.9	0.999	0.46	1.2
<i>cis</i> -aconitate	0.5	7.2	0.997	0.12	4.4
3-phosphoglycerate	0.5	4.9	0.995	0.19	2.8
isocitrate	0.5	3.6	0.996	0.19	6.0
citrate	0.5	7.3	0.988	0.09	63
gluconate	0.7	5.1	0.999	1.1	0.8
E4P	0.6	6.0	0.999	0.81	2.1
Ru5P	0.6	2.7	0.999	0.21	2.4
R5P	0.6	5.1	0.999	0.26	1.9
G1P	0.6	2.1	0.983	0.15	1.9
F6P	0.6	3.5	0.980	0.19	3.4
G6P	0.6	2.4	0.992	0.16	1.6
2,3DPG	0.5	5.8	0.997	0.13	35
6-phosphogluconate	0.5	5.4	0.999	0.18	2.9
F1,6P	0.5	5.4	0.999	0.17	3.1
AMP	0.7	3.5	0.999	0.11	2.1
IMP	0.7	4.8	0.999	0.11	2.9
GMP	0.7	3.6	0.999	0.09	2.0
NADPH ^b	0.6	4.3	0.990	0.45	2.7
CoA ^b	0.6	6.1	0.994	0.03	nc ^c
acetyl CoA ^b	0.6	5.2	0.999	0.04	5.2
malonyl CoA ^b	0.6	6.6	0.995	0.05	7.6
ADP	0.6	3.9	0.995	0.06	5.3
succinyl CoA ^b	0.6	12.1	0.996	0.15	10
GDP	0.6	5.6	0.996	0.11	5.5
UTP	0.6	3.4	0.999	0.10	7.8
ATP	0.6	5.8	0.999	0.22	6.6
GTP	0.6	14.4	0.989	0.10	15
NAD	1.1	4.8	0.999	0.11	1.8
NADH	0.7	3.4	0.999	0.49	11
NADP	0.7	6.1	0.999	0.10	2.4
FAD	0.8	10.5	0.999	0.12	2.8

^a Improved sensitivity was calculated by dividing the detection limit with the SST316Ti stainless steel by that with the platinum needle. ^b Detected at the divalent [M - 2H]²⁻ ion. ^c nc, not calculated. Improved sensitivity of CoA was not calculated because CoA was not determined by the SST316Ti stainless steel.

isopropanol aqueous solution at 80 °C for 30 min) and platinum. Metal amounts in run buffer solution in the inlet vial and separation capillary were determined using an Agilent 7500 inductivity coupled plasma mass spectrometer (Tokyo, Japan). For the capillary analysis, the polyimide coating was burned with a lighter and removed with methanol, and then the capillary was cut into five pieces (each 20 cm). Each capillary (5.4 mg) was dissolved by ultrasonic treatment in 8 mL of 38% hydrofluoric acid for 80 min, and this solution was used for the inductivity coupled plasma mass spectrometry (ICP-MS) analysis.

CE-TOFMS Conditions for Anionic Metabolite Analysis.

A commercially available COSMO(+), chemically coated with a cationic polymer, capillary (50 μm i.d. × 110 cm) (Nacalai Tesque, Kyoto, Japan) was used as the separation capillary. A 50 mM ammonium acetate solution (pH 8.5) was the electrolyte for CE separation. Prior to the first use, a new capillary was flushed successively with the running electrolyte, 50 mM acetic acid (pH 3.4), and then the electrolyte again for 20 min each. Before each

injection, the capillary was equilibrated for 2 min by flushing with 50 mM acetic acid (pH 3.4) and then for 5 min by flushing with the running electrolyte.²⁰

A sample solution (30 nL) was injected at 50 mbar for 30 s, and -30 kV of voltage was applied. The capillary temperature was thermostated to 20 °C, and the sample tray was cooled to below 5 °C. The Agilent 1100 series pump equipped with a 1:100 splitter was used to deliver 10 μL/min of 5 mM ammonium acetate in 50% (v/v) methanol-water containing 0.1 μM Hexakis to the CE interface where it is used as a sheath liquid around the outside of the CE capillary to provide a stable electrical connection between the tip of the capillary and the grounded electrospray needle.

ESI-TOFMS was conducted in the negative ionization; the capillary voltage was set at 3500 V. For TOFMS, the fragmenter, skimmer, and Oct RFV voltage was set at 100, 50, and 200 V, respectively. A flow rate of drying nitrogen gas (heater temperature, 300 °C) was maintained at 7 L/min. Automatic recalibration

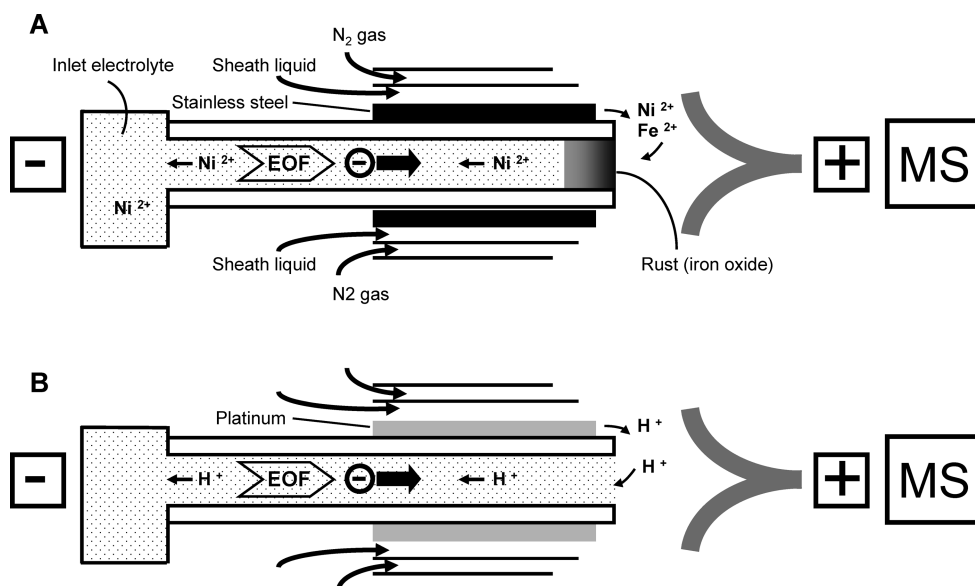


Figure 2. Schematic of anion analysis by the CE-MS in the negative mode using the CE-ESI-MS sprayer with (A) the stainless steel needle and (B) the platinum needle. (A) Metal ions like Fe^{2+} and Ni^{2+} were electrochemically generated from the stainless steel needle at the anode (pH 6.9) and moved into the separation capillary. Fe^{2+} was oxidized (forming rust) and plugged at the capillary outlet due to high electrolyte pH (8.5), while Ni^{2+} migrated toward the capillary inlet (cathode). Anions exhibiting high chelating properties with metal ions formed complexes when encountering Ni^{2+} or iron oxides. (B) In the platinum needle, water oxidation ($2\text{H}_2\text{O} \rightarrow 4\text{H}^+ + \text{O}_2\uparrow + 4\text{e}^-$) occurred at the anode and, thus, anionic metabolites did not encounter the metal ions.

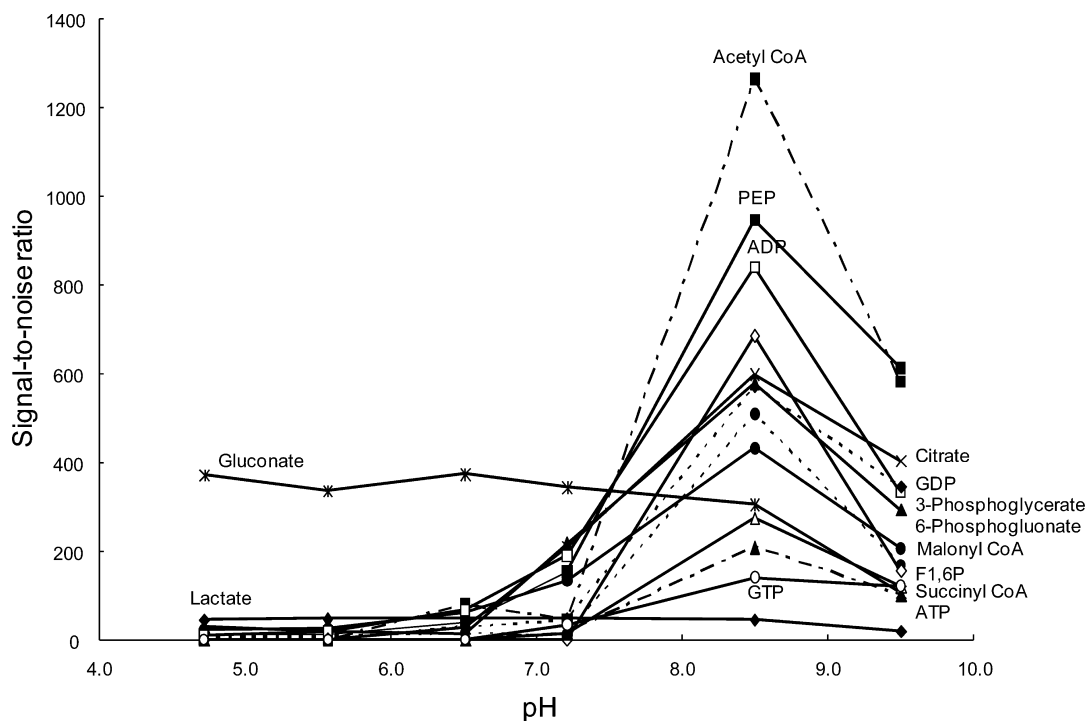


Figure 3. Effect of electrolyte pH on the sensitivity (signal-to-noise ratio) of anions. Experimental conditions: ESI spray needle, platinum; electrolyte, 50 mM ammonium acetate; other experimental conditions as in Figure 1.

of each acquired spectrum was performed using reference masses of reference standards ($[\text{C}^{13}\text{isotopic ion of deprotonated acetic acid dimer } (2\text{CH}_3\text{COOH} - \text{H})^-]$, m/z 120.03841), and ($[\text{Hexakis} + \text{deprotonated acetic acid } (\text{CH}_3\text{COOH} - \text{H})^-]$, m/z 680.03554). Exact mass data were acquired at a rate of 1.5 spectra/s over a 50–1000 m/z range.

Raw CE-TOFMS data were processed using software developed in-house for the quantification of metabolites.^{13,25,26} All target

metabolites were identified by matching their m/z values and migration times with those of standard compounds. For overall data analysis, three-dimensional representation of CE-TOFMS data was produced using MZmine2 software^{27,28} (<http://mzmine.sourceforge.net/>).

(25) Baran, R.; Kochi, H.; Saito, N.; Suematsu, M.; Soga, T.; Nishioka, T.; Robert, M.; Tomita, M. *BMC Bioinf.* **2006**, *7*, 530.

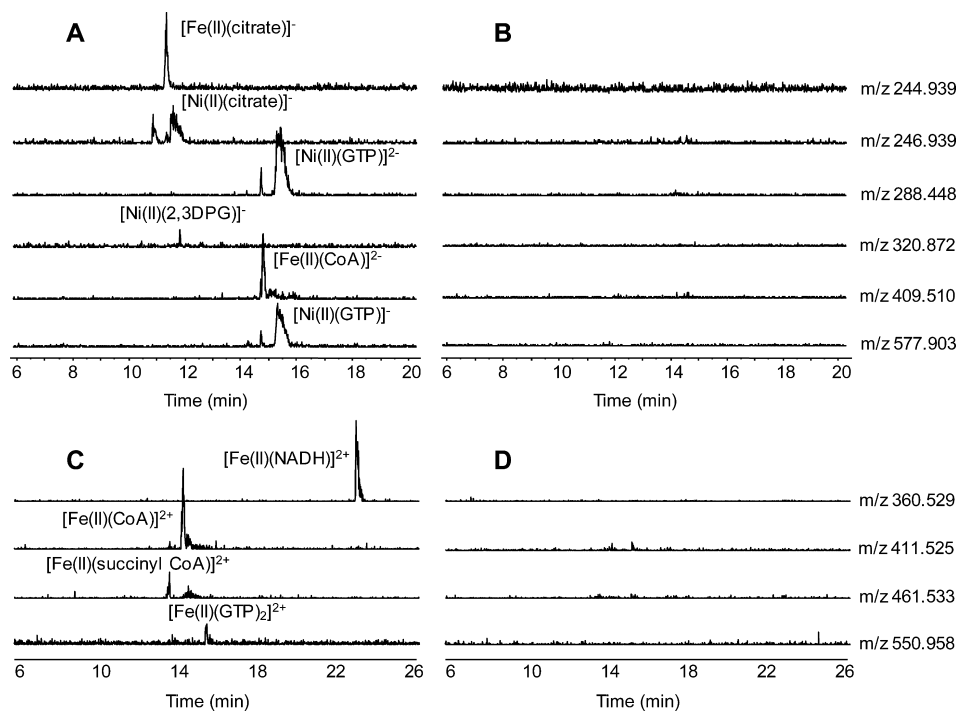


Figure 4. Abundance of metal–anion complexes in the analysis of 43 anionic metabolite standards using CE-TOFMS in the negative mode and negative ionization detection with (A) the stainless steel needle and (B) the platinum needle and positive ionization detection with (C) the stainless steel needle and (D) the platinum needle. Experimental conditions: the names of 43 anionic metabolite standards are listed in Table 1; the standard concentration was 50 μ mol/L each; in the positive TOFMS detection, the ion polarity was switched to positive and the capillary voltage was set at 4000 V; other experimental conditions are the same as in Figure 1.

RESULTS AND DISCUSSION

Prevention of Capillary Plugging by Use of a Platinum ESI Needle. The sheath flow CE-MS method with negative mode using a cationic polymer-coated capillary demonstrated impressive performance for anion analysis.^{13,20} However, the sensitivities of several anions were considerably poor. Moreover, migration times of every analyte immediately became longer, and the capillary frequently clogged. Removing the polyimide film, we examined a clogged capillary using a microscope and found that the capillary outlet became plugged with a rustlike precipitate. To identify it, we investigated its solubility using several organic solvents and acids including chloroform, isopropanol, acetone, acetonitrile, hydrochloric acid, hydronitric acid, and hydrosulfuric acid. Since it was only soluble in hydrochloric acid, it was identified as a transition metal having a high ionization tendency like iron and nickel.

Although the original Agilent CE-ESI-MS spray needle is made from SST316Ti stainless steel, it exhibited high ionization tendency and, thus, was oxidized to metal ions by electrolysis, resulting in a plug at the capillary outlet. To confirm this, we attached the following three types of spray needles to the Agilent ESI sprayer: normal- and passivated-SST316Ti stainless steel and platinum. Using these spray needles, we performed the CE-MS analyses with the negative mode and checked the capillary outlet with a microscope after 5, 10, and over 40 runs, respectively.

With the two needles made from the stainless steel, both the capillary outlets became plugged with precipitates (rust) after five runs and the rust grew thicker with the number of analysis performed, indicating that electrochemical oxidation of the stainless steel occurred. However, the use of the platinum needle resulted in no plugging for 100 runs. This is consistent with previous reports that platinum wire used as the CE-MS ESI electrode protects against electrode corrosion.^{29–32} As Smith and Moini³¹ reported, when a stainless steel wire was used as the anode, the oxidation of iron ($\text{Fe} \rightarrow \text{Fe}^{2+} + 2\text{e}^-$) (perhaps Ni, Cr, and Ti) replaced the oxidation of water ($2\text{H}_2\text{O} \rightarrow 4\text{H}^+ + \text{O}_2\uparrow + 4\text{e}^-$) by electrolysis, resulting in corrosion of the Fe and formation of Fe^{2+} . However, platinum wire only caused electrochemical oxidation of water, and bubble formation occurred at the anodic end.

The robustness of the CE-MS method with the negative mode using the SST316Ti stainless steel needle and platinum needle was further investigated. With the stainless steel needle, both capillary clogging with rust and significant corrosion at the tip of the needle occurred (Figure 1A) and the current fully dropped after 167 runs (Figure 1C). For the platinum needle, although a slight current drop and migration time fluctuation were observed (Figure 1C), it enabled over 545 successive analyses without capillary clogging and corrosion of the needle (Figure 1B). While Smith and Moini used iron wire, instead of platinum wire, as the anode to eliminate gas bubble formation in their sheathless CE-

(26) Hirayama, A.; Kami, K.; Sugimoto, M.; Sugawara, M.; Toki, N.; Onozuka, H.; Kinoshita, T.; Saito, N.; Ochiai, A.; Tomita, M.; Esumi, H.; Soga, T. *Cancer Res.* **2009**, *69*, 4918–4925.

(27) Katajamaa, M.; Oresic, M. *BMC Bioinf.* **2005**, *6*, 179.

(28) Katajamaa, M.; Miettinen, J.; Oresic, M. *Bioinformatics* **2006**, *22* (5), 634–636.

(29) Cao, P.; Moini, M. *J. Am. Soc. Mass Spectrom.* **1997**, *8*, 561–564.

(30) Herring, C. J.; Qin, J. *Rapid Commun. Mass Spectrom.* **1999**, *13*, 1–7.

(31) Smith, A. D.; Moini, M. *Anal. Chem.* **2001**, *73*, 240–246.

(32) Van Berkel, G. J.; Asano, K. G.; Schnier, P. D. *J. Am. Soc. Mass Spectrom.* **2001**, *12*, 853–862.

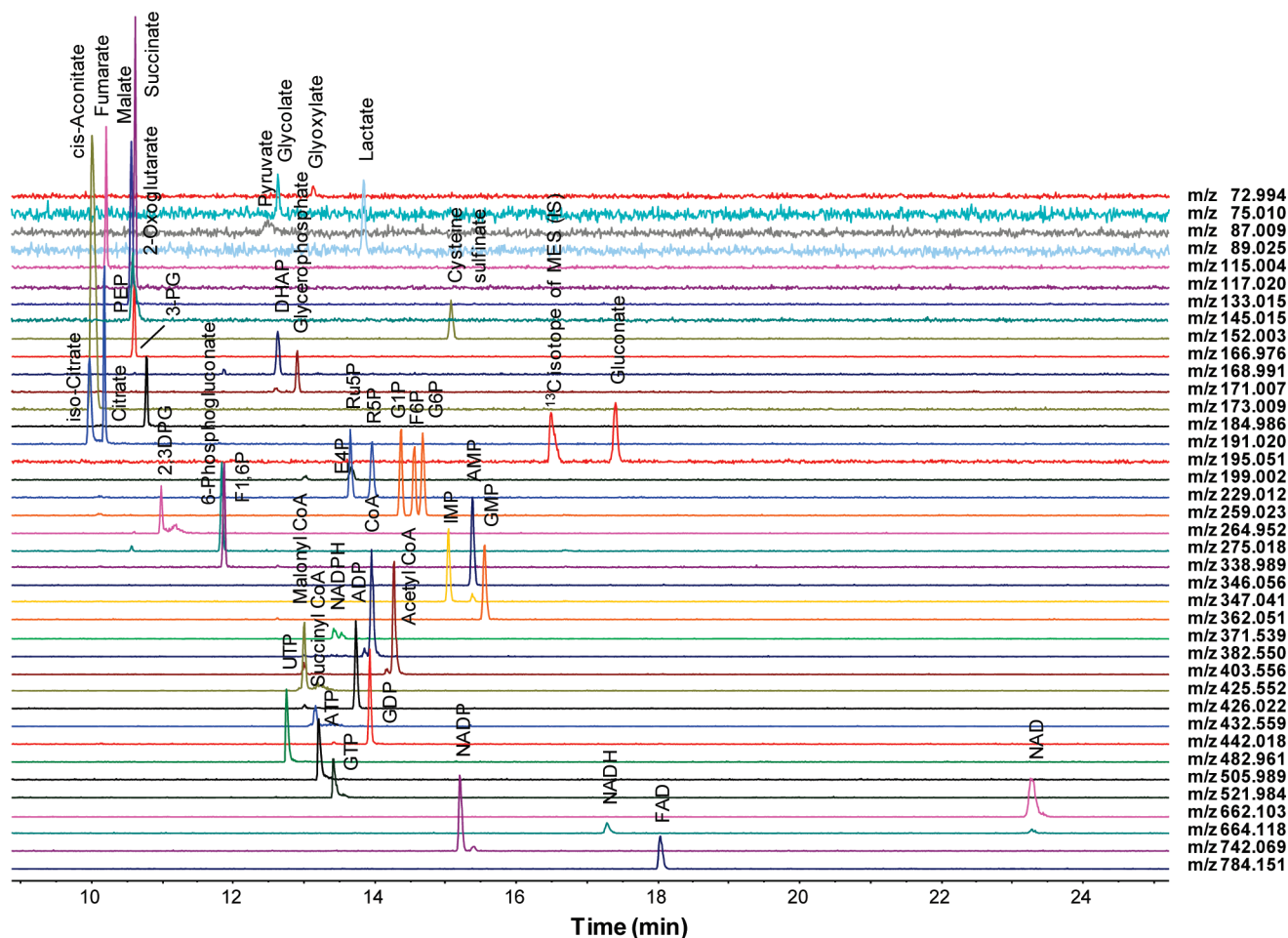


Figure 5. Selected CE-TOFMS ion electropherograms for a standard mixture of anionic metabolites in the components of glycolysis, pentose phosphate, and the TCA pathways obtained by the CE-ESI-MS sprayer attached with a platinum needle. Experimental conditions: standard concentration, 10 $\mu\text{mol/L}$ each; other experimental conditions as in Figure 1. Abbreviations: PEP, phosphoenolpyruvate; DHAP, dihydroxyacetone phosphate; 3PG, 3-phosphoglycerate; E4P, erythrose 4-phosphate; Ru5P, ribulose 5-phosphate; R5P, ribose 5-phosphate; G1P, glucose 1-phosphate; F6P, fructose 6-phosphate; G6P, glucose 6-phosphate; 2,3DPG, 2,3-diphosphoglycerate; F1,6P, fructose 1,6-diphosphate; NADPH, reduced nicotinamide adenine dinucleotide phosphate; NADP, nicotinamide adenine dinucleotide phosphate; FAD, flavin adenine dinucleotide.

MS system,³¹ our results indicate that bubble formation generated by the platinum needle had no effect on the analysis in the sheath flow CE-MS system.

Sensitivity Differences between the Stainless Steel Needle and the Platinum Spray Needle in Anion Analysis. There was another difficulty in analyzing anionic metabolites by the CE-MS method with the negative mode using the ESI sprayer equipped with the SST316Ti stainless steel needle. Several carboxylic acids and phosphorylated compounds such as malate, 2-oxoglutarate, 3-phosphoglycerate (3PG), citrate, isocitrate, gluconate, 2,3-diphosphoglycerate (2,3DPG), uridine 5'-triphosphate (UTP), adenosine 5'-triphosphate (ATP), guanosine 5'-triphosphate (GTP), reduced nicotinamide adenine dinucleotide (NADH), coenzyme A (CoA), and acetyl- and malonyl-CoA with a concentration below a few micromolar were not detected. However, all the anions were detected as well-defined peaks with the platinum needle.

Many carboxylic acids and nucleotides such as citrate, malate, ATP, GTP, and NADH are complexing agents,^{33–38} which display high stability constants for transition metals. For phosphorylated

saccharides and CoAs, stability constants for transition metals have not been frequently reported. However, as metal–phosphate affinity is well-known^{33,35,39,40} and these characteristics are frequently utilized in phosphoproteomics studies,^{41,42} most phosphorylated compounds will likely interact with transition metals.

Experiments show sensitivity differences between the two needles for metal-chelating carboxylic acids, and phosphorylated anions are observed (Table 1). Conversely, pyruvate, lactate, and fumarate exhibit little or no stability constants for transition metals,³⁴ and their sensitivities were independent of the needle type. Unlike NADH, nicotinamide adenine dinucleotide (NAD^+)

(35) Kowaltowski, A. J.; Vercesi, A. E. *Free Radical Biol. Med.* **1999**, *26*, 463–471.

(36) Canaviri, E. C.; Feliz, M. R.; Capparelli, A. L. *Transition Met. Chem.* **1992**, *17*, 446–448.

(37) Champeil, P.; Rigaud, J. L.; Gary-Bobo, C. M. *Proc. Natl. Acad. Sci. U.S.A.* **1980**, *77*, 2405–2409.

(38) Lvovich, V.; Scheeline, A. *Arch. Biochem. Biophys.* **1995**, *320*, 1–13.

(39) Takebayashi, Y.; Mitsuma, R.; Imanari, T. *Anal. Sci.* **1987**, *3*, 569–572.

(40) Ziemiak, S. E.; Jones, M. E.; Combs, K. E. S. *J. Solution Chem.* **1989**, *18*, 1133–1152.

(41) Stensballe, A.; Andersen, S.; Jensen, O. N. *Proteomics* **2001**, *1*, 207–222.

(42) Kokubu, M.; Ishihama, Y.; Sato, T.; Nagasu, T.; Oda, Y. *Anal. Chem.* **2005**, *77*, 5144–5154.

(33) Toyokuni, S. *Free Radical Biol. Med.* **1996**, *20*, 553–566.

(34) Soga, T.; Gordon, R. A. *J. Chromatogr. A* **1997**, *767*, 223–230.

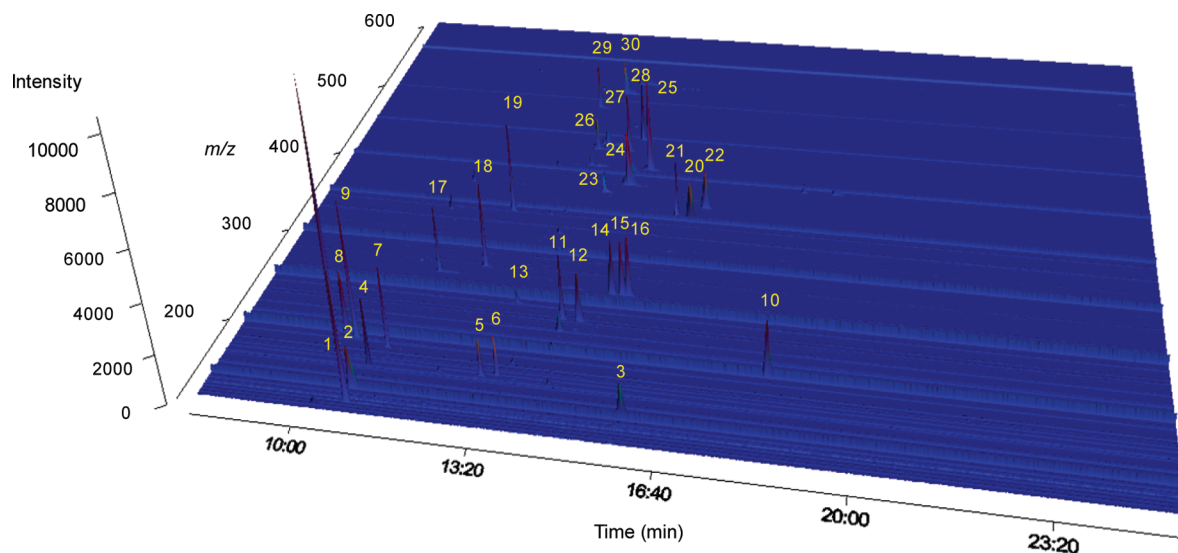


Figure 6. Three-dimensional representation (total ion electropherogram) for the analysis of a standard mixture of anionic metabolites found in glycolysis, pentose phosphate, and the TCA pathways. Results were obtained by the CE-TOFMS in the negative mode using the CE-ESI sprayer with a platinum needle. Experimental conditions: standard concentration, 50 $\mu\text{mol/L}$ each; other experimental conditions are the same as in Figure 1. Peaks: 1, malate; 2, 2-oxoglutarate; 3, cysteine sulfinate; 4, PEP; 5, DHAP; 6, glycerophosphate; 7, 3PG; 8, isocitrate; 9, citrate; 10, gluconate; 11, E4P; 12, Ru5P; 13, R5P; 14, G1P; 15, F6P; 16, G6P; 17, 2,3DPG; 18, 6-phosphogluconate; 19, F1,6P; 20, AMP; 21, IMP; 22, GMP; 23, NADPH; 24, CoA; 25, acetyl CoA; 26, malonyl CoA; 27, ADP; 28, GDP; 29, UTP; 30, ATP.

does not form a complex with the Fe^{2+} ion;³⁸ thereby, NAD^{+} 's sensitivity is most similar between the two needles. These facts indicate that the anions' metal-chelating properties likely affect their detection sensitivities.

Effect of Generated Metal Ions on Sensitivity in Measurement of Anionic Metabolites. To investigate the hypothesis that anionic metabolites exhibiting high stability constants for metal ions might form complexes with the iron oxides generated by the stainless steel needle, the separation capillary was cut into five pieces (each 20 cm) and analyzed by ICP-MS. The ICP-MS analysis detected a 10.4 ppb level of Fe in the tip of the capillary outlet (the anode side), which identified the rust as iron oxide, but no metals in other regions of the capillary. Surprisingly, nickel was detected in the capillary inlet electrolyte, and its concentration dramatically increased (0.96 $\mu\text{g/L}$ at 1 h and reached 3.08 $\mu\text{g/L}$ at 2 h) even when no sample was injected. This indicates that nickel ion migrated from the anode to the inlet electrolyte vial. However, no such phenomena were observed when using the platinum needle.

It is, therefore, assumed that, with the stainless steel needle (Figure 2A), iron and nickel ions generated at the anode due to electrolysis moved to the capillary outlet in the sheath liquid (pH 6.9) and iron oxides formed because of the high pH (pH 8.5)²⁰ (Figure 3). Simultaneously, Ni^{2+} ions migrated toward the cathode without precipitation and then collected in the capillary inlet electrolyte vial. In this manner, injected anionic metabolites encountered Ni^{2+} in the separation capillary or the iron oxides at the capillary end and formed metal-anion complexes (Figure 2A). In the case of the platinum needle, water oxidation ($2\text{H}_2\text{O} \rightarrow 4\text{H}^+ + \text{O}_2\uparrow + 4\text{e}^-$) occurred at the anode due to its low ionization tendency and anionic metabolites did not encounter the metal ions and were fully detected by the mass spectrometer (Figure 2B).

The formation of metal-anion complexes during the CE-MS analysis was also confirmed. As listed in Table 1, when the stainless steel needle was used, a significant drop in sensitivity was observed for many anions including citrate, 2,3DPG, GTP, CoA, succinyl CoA, and NADH. For these anions, the formation of all nickel(II)- and iron(II)-anion complexes was analyzed by the CE-TOFMS method. In the negative ionization TOFMS method, nickel(II)- and iron(II)-anion complexes such as $[\text{Fe}(\text{II})-(\text{citrate})]^-$, $[\text{Ni}(\text{II})-(\text{citrate})]^-$, $[\text{Ni}(\text{II})-(\text{GTP})]^{2-}$, $[\text{Ni}(\text{II})-(2,3\text{DPG})]^-$, $[\text{Fe}(\text{II})-(\text{CoA})]^{2-}$, and $[\text{Ni}(\text{II})-(\text{GTP})]^-$ were detected with the stainless steel needle (Figure 4A). Moreover, positively charged nickel(II)- and iron(II)-anion complexes such as $[\text{Fe}(\text{II})-(\text{NADH})]^{2+}$, $[\text{Fe}(\text{II})-(\text{CoA})]^{2+}$, $[\text{Fe}(\text{II})-(\text{succinyl CoA})]^{2+}$, and $[\text{Fe}(\text{II})-(\text{GTP})_2]^{2+}$ were present in the positive ionization TOFMS detection (Figure 4C). These results indicate that all the anions formed complexes with nickel(II) and iron(II) ions with the stainless steel needle. No metal complexes were observed with the platinum needle (Figure 4B,D).

It was found, however, that the sensitivities for pyruvate, lactate, and fumarate were equivalent using either the stainless steel or platinum needle (Table 1). Although a trace of $[\text{Fe}(\text{II})-(\text{pyruvate})_3]^-$ was detected with the stainless steel needle, neither these nickel(II)- nor iron(II)-anion complexes were detected with either needle. These results indicate that with the stainless steel needle, anions exhibiting high stability constants with metals formed complexes with nickel and iron ions generated by electrolysis, resulting in a significant decrease in detection sensitivity.

Effect of Electrolyte pH on Rust Formation and Sensitivity in the CE-MS System. Given that iron ions generated from the stainless steel needle precipitated when encountering the alkaline electrolyte (pH 8.5), they are expected to be dissolved under acidic conditions. To confirm this, iron oxide formation was studied over

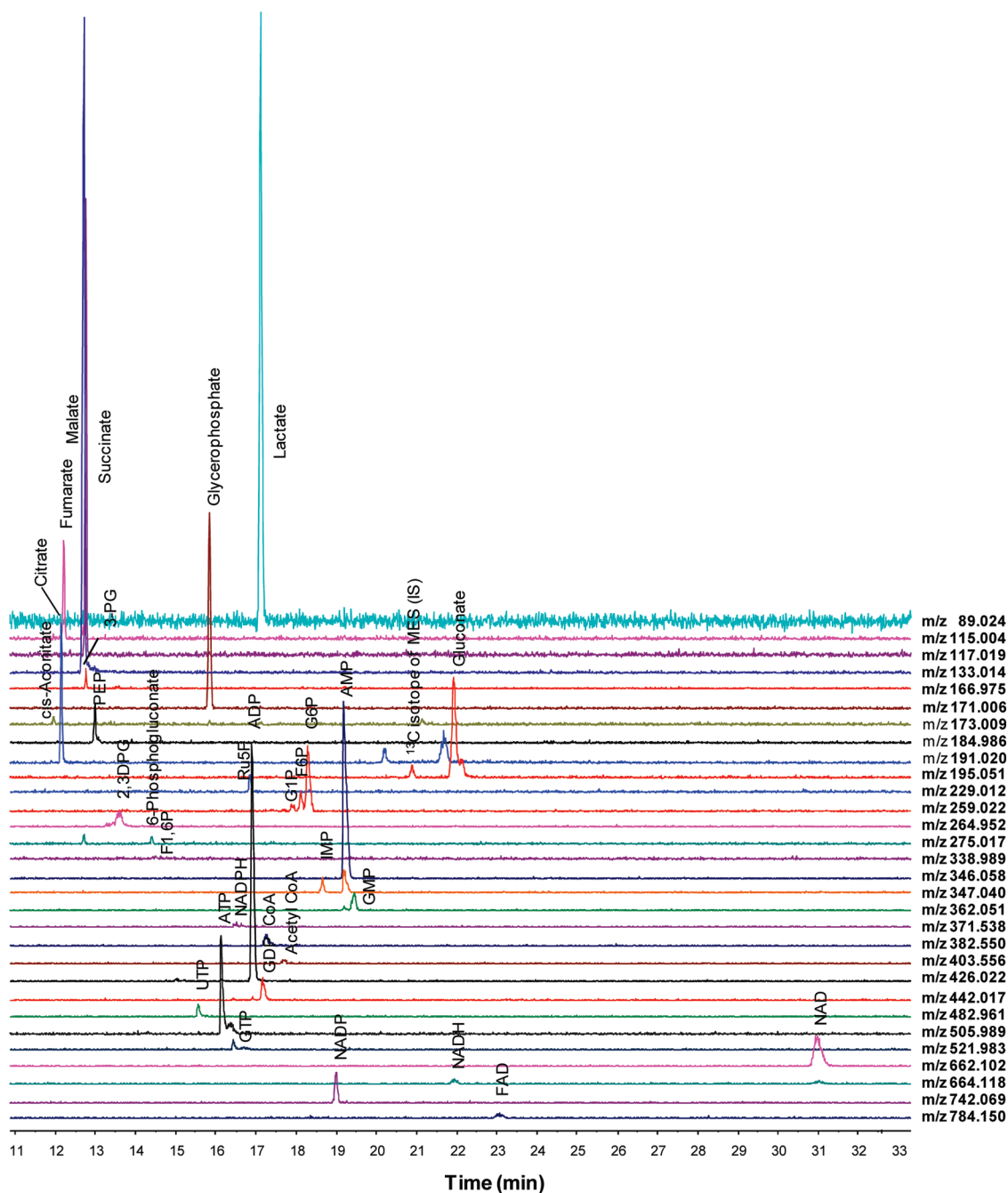


Figure 7. Selected CE-TOFMS ion electropherograms for components of glycolysis, pentose phosphate, and the TCA pathways in mouse liver. Experimental conditions are the same as in Figure 1.

pH range 4.7–9.5 using 50 mM ammonium acetate as the electrolyte and the stainless steel needle. At a pH value of 7.5, both rust development at the capillary end and corrosion of the stainless steel needle were observed. At pH 5.0, although corrosion of the needle was still observed, no iron oxide was formed. After the voltage was applied (no sample injection) for 2 h at the pH 5.0, metals at the capillary inlet electrolyte were analyzed by ICP-MS. Fe, Ni, and Ti, some components of the SST316Ti stainless steel, were detected at amounts of 1.23, 0.88, and 0.24 $\mu\text{g/L}$, respectively, which strongly implies that these metal ions were generated by electrolysis and migrated toward the cathodes.

Nevertheless, decreasing electrolyte pH had a significant effect on the detection sensitivity of anionic species (Figure 3). Below pH 7.5, although the reason was unclear, a considerable deteriora-

tion in the peak shape and extended migration time of many anions including phosphorylated substrates, nucleotide di- and triphosphates, and CoAs were observed, which resulted in substantial reduction in their detection sensitivity. Particularly, neither nucleotide triphosphates nor CoAs were detected below pH 6.5. Sensitivities of anions also decreased when the pH was increased to pH 9.5. Maximal sensitivities for most anions were obtained at pH 8.5 (Figure 3). This result was independent of the ESI needle type used. Reduction of sensitivity depending on the pH may be caused by the interaction between these compounds and the cationic coated polymer on the capillary wall, though further investigation is necessary.

In conclusion, there is no pH that can be used with the stainless steel needle to both prevent iron oxide formation and maintain

Table 2. Metabolite Amount, Reproducibility, and Recovery in Mouse Liver Analysis

compound	amount (nmol/g)	RSD (<i>n</i> = 12) (%)	recovery rate (average, <i>n</i> = 5) (%)
glyoxylate	nd ^a		106
glycolate	nd		117
pyruvate	nd		138
lactate	2440	5.7	67
fumarate	247	8.4	99
succinate	526	4.9	65
malate	1250	2.6	53
2-oxoglutarate	nd		94
cysteine sulfinate	nd		101
PEP	44	7.8	96
DHAP	nd		100
glycerophosphate	1310	3.9	97
<i>cis</i> -aconitate	247	15.6	141
3-phosphoglycerate	159	5.0	103
isocitrate	nd		103
citrate	264	6.1	89
gluconate	675	4.5	109
E4P	nd		114
Ru5P	68	11.1	101
R5P	nd		98
G1P	34	12.7	97
F6P	98	7.0	92
G6P	392	4.7	95
2,3DPG	215	5.1	93
6-phosphogluconate	23	21.9	97
F1,6P	22	15.8	92
AMP	1240	2.1	96
IMP	81	7.9	98
GMP	143	4.8	93
NADPH (divalent)	66	16.5	146
CoA (divalent)	68	10.0	132
acetyl CoA (divalent)	14	15.4	96
malonyl CoA (divalent)	nd		110
ADP	1500	4.7	88
succinyl CoA (divalent)	nd ^a		58
GDP	181	3.0	94
UTP	89	15.3	94
ATP	889	3.8	120
GTP	149	6.2	183
NAD	494	3.7	93
NADH	166	7.2	114
NADP	184	4.9	90
FAD	47	7.5	92

^a nd, not detected.

peak shape for necessary detection sensitivity. For the platinum needle, pH 8.5 was found optimal.

Method Validation. Figure 5 illustrates selected ion electropherograms of the 43 anionic metabolite standards in the components of glycolysis, pentose phosphate, and the tricarboxylic acid (TCA) pathways obtained by the sheath flow CE-TOFMS with the negative mode using the platinum spray needle. A three-dimensional presentation (total ion electropherogram) is shown in Figure 6. This analysis will be particularly important to analyze unknown metabolites. This approach provided much better sensitivity and, thereby, contributed to excellent performance, compared to the previous method. Most of compounds were detected at their monovalent deprotonated molecular $[M - H]^-$ ions, while intensity in the divalent $[M - 2H]^{2-}$ ion of NADPH and CoA compounds was higher than that in monovalent ion.

The reproducibility, linearity, and sensitivity of this method are listed in Table 1. Practical reproducibility was obtained for all anionic species with relative standard deviation (RSD) values (*n* = 8) for migration times between 0.5 and 1.1 min and for peak areas

better than 10% except for glyoxylate, glycolate, succinyl CoA, GTP, and FAD, as indicated in the table. The calibration curves for all species were linear at 1, 2, 5, 10, 20, 50, 100, and 200 $\mu\text{mol/L}$ with correlation coefficients between 0.980 and 0.999.

This method significantly improved the sensitivity of many anions. Although the previous method using the stainless steel needle was unable to detect 20 $\mu\text{mol/L}$ of CoA, the use of the platinum needle dramatically improved sensitivity and enabled the detection of 1 $\mu\text{mol/L}$ of CoA. Moreover, the sensitivities for the anions exhibiting high stability constants for metal ions such as citrate, 2,3DPG, GTP, and NADH were 63-, 35-, 15-, and 11-fold superior to those obtained by the stainless steel needle, respectively. Also several-fold better sensitivities for many anions including malate, 2-oxoglutarate, *cis*-aconitate, isocitrate, ADP, ATP, GDP, UTP, and succinyl-, acetyl-, and malonyl CoA were obtained.

Anions exhibiting low stability constants with metals such as pyruvate and lactate showed similar sensitivities between the two needles. Overall, the concentration detection limits for most of the anions, except for glyoxylate, glycolate, pyruvate, and lactate, were between 0.03 and 1.1 $\mu\text{mol/L}$ with a pressure injection of 50 mbar for 30 s (30 nL); i.e., mass detection limits ranged from 0.8 to 33 fmol, at a signal-to-noise ratio of 3.

Analysis of Mouse Liver Metabolites in the Central Carbon and Energy Metabolism. The utility of the CE-TOFMS method was demonstrated by the simultaneous analysis of the central carbon and energy metabolism components extracted from mouse liver. There are more than 40 anionic intermediates that belong to several categories of chemical compounds: phosphorylated saccharides, phosphorylated carboxylic acids, carboxylic acids, nucleotides, and cofactors. Simultaneous, quantitative, and direct analysis of these compounds is a challenging analytical problem. Figure 7 shows the results for the analysis of the central carbon and energy metabolic components extracted from mouse livers obtained by the CE-TOFMS method. The 32 components were identified by comparing their molecular weights and migration times with those of metabolite standards, and their amounts were quantified by their standard calibration curves (Table 1). The relative standard deviations (*n* = 12) for the amounts of identified compounds in the mouse liver sample were better than 6% except for small compounds. To investigate quantification accuracy and ion suppression effect in this system, we analyzed mouse liver samples spiked with 20 μM of each standard and calculated the recovery (Table 2). Except for a few metabolites, the recovery rates of most metabolites in the CE-TOFMS approach were between 80 and 130%. Although the reason was not clear, the recovery rate of GTP was unusually high (183%). Considering the good reproducibility and recovery rates, the CE-TOFMS method in the negative mode using the platinum spray needle seems to be scarcely affected by the ion suppression effect and it enables sufficient quantitative analysis of most anionic intermediates in the central carbon and energy metabolic pathways extracted from mouse liver samples.

CONCLUSIONS

A negatively charged metabolites profiling approach based on sheath flow CE-TOFMS with a negative mode is described. The material of the ESI spray needle had a significant effect

on the measurement of anions. Due to electrolysis, the stainless steel sprayer needle was easily oxidized and generated metal ions, which caused corrosion of the needle and capillary clogging. Moreover, metal ions formed complexes with many anions, significantly decreasing detection sensitivity. The key to success was using a platinum spray needle, a low ionization tendency metal, which prevented both generation of metal ions and corrosion of the needle caused by electrolysis. Compared with the previously reported techniques, this method has several advantages: (1) it is able to integrate two CE-MS methods into one method, and thereby, all types of anionic components such as phosphorylated saccharides, phosphorylated carboxylic acids, carboxylic acids, CoA compounds, nucleotides, and nicotinamide adenine dinucleotides are simultaneously analyzed; (2) more than several-fold increased sensitivities of anions which exhibit high metal chelating properties are obtained; and (3) the present method provides improved reproducibility, quantification accuracy, and method robustness (i.e., capillary lifetime). Its utility was demonstrated by the simultaneous and quantitative analysis of the central carbon and the energy the metabolic intermediates extracted from mouse livers. These results indicate that the proposed CE-TOFMS method can be useful for the comprehensive analysis of anionic species in a wide range of application areas.

ACKNOWLEDGMENT

We thank Akiyoshi Hirayama and Dr. Masahiro Sugimoto, Institute for Advanced Biosciences, Keio University, and Takamasa Ishikawa, Human Metabolome Technologies Inc., for technical support, and Dr. David N. Heiger, Agilent Technologies, for critical reading of the manuscript. This work was supported in part by grants for the Health and Labour Sciences Research Grants entitled "Research on Risk of Chemical Substances" and "Research on Biological Markers for Drug development", by a Grant-in-Aid for Creative Scientific Research 17GS0419 from the Japan Society for the Promotion of Science, by a grant from the Global COE Program entitled "Human Metabolic System Biology", and by a Grant-in-Aid for Scientific Research on Priority Areas "Life surveyor" and "Systems Genomes" from the Ministry of Education, Culture, Sport, Science, and Technology (MEXT) in Japan as well as by research funds from Yamagata prefectural government and Tsuruoka city.

Received for review March 31, 2009. Accepted May 31, 2009.

AC900675K